ISSN (Online) 2456-1290
International Journal of Engineering Research in Mechanical and Civil Engineering (IJERMCE)
Volume 13, Issue 06, June 2026

Flood Susceptibility and Risk Assessment of Kolhapur District, Maharashtra, India: An Integrated GIS and Remote Sensing Approach Using Multi-Criteria Spatial Analysis

[1] Saurabh Ravindra Torase, [2] Srushti Krishnakumar Mendhe

[1] Post Graduate Student Department of Planning COEP Technological University Pune, Maharashtra, India
[2] Faculty Department of Planning COEP Technological University Pune, Maharashtra, India
Corresponding Author Email: [1] saurabh.torase@gmail.com

Abstract— ***Flood events represent one of the most devastating natural hazards in India, with the Kolhapur district of Maharashtra being particularly vulnerable due to its complex topography, intense monsoonal rainfall, and rapidly expanding urban footprint. This study presents a comprehensive geospatial assessment of flood susceptibility and flood risk across Kolhapur district by integrating four key biophysical and socio-demographic parameters: mean annual rainfall, terrain slope, urban density, and population count. A multi-criteria weighted index approach was employed wherein flood susceptibility was computed as a normalised composite of rainfall erosivity and slope gradient, while flood risk was derived by coupling susceptibility with population exposure and urban density. Spatial data were processed and analysed using Python-based geospatial libraries (rasterio, numpy, matplotlib) operating on high-resolution raster datasets. Results reveal that flood susceptibility values across the district range predominantly between 0.3 and 0.7 (mean ≈ 0.45), with the highest susceptibility concentrated in the northwestern and central urban zones where low slopes intersect with high monsoonal rainfall. Flood risk, after incorporating population and urban density weights, is highly skewed towards near-zero values for the majority of the district, while a spatially concentrated nucleus of high risk (index > 0.4) is evident in and around the Kolhapur Municipal Corporation area. Quantile-based classification identifies approximately 30% of non-zero pixels as moderate-to-high risk. Scatter plot diagnostics confirm that flood risk exhibits a non-linear threshold response to flood susceptibility, activating sharply around a susceptibility value of 0.62–0.65, which corresponds to zones of peak population density and near-complete urban coverage. These findings have direct implications for urban flood management planning, early warning system design, and infrastructure investment prioritisation in Kolhapur.***

Keywords— ***Flood susceptibility, flood risk index, geospatial analysis, urban density, rainfall, population exposure.***

I. INTRODUCTION

Floods are among the most recurrent and destructive natural hazards globally, accounting for approximately 40% of all natural disaster events and affecting millions of people annually (UNDRR, 2020). In the Indian subcontinent, floods cause significant loss of life, agricultural damage, and urban infrastructure disruption every monsoon season. Maharashtra, positioned along the windward slopes of the Western Ghats, receives some of the highest rainfall intensities in South Asia, making districts such as Kolhapur especially prone to catastrophic flood events. The 2019 and 2021 Kolhapur floods, which inundated large portions of the urban core and adjacent agricultural zones, underscored the pressing need for systematic, spatially explicit flood risk assessment that integrates both natural hazard drivers and socio-demographic vulnerability.

Traditional flood mapping approaches have relied heavily on hydrological modelling, stream gauge records, and engineering surveys. While robust, these methods are data-intensive, computationally demanding, and often inaccessible to district-level planners in developing countries. The advent of open-source geospatial tools, freely available satellite-derived datasets, and high-performance computing has opened new avenues for rapid, scalable flood risk assessment (Tehrany et al., 2014; Rahmati et al., 2016).

Flood susceptibility modelling identifies areas where physical conditions favour flood occurrence, including low-gradient topography, high rainfall intensity, impervious surfaces, and proximity to water bodies (Pradhan, 2010; Khosravi et al., 2016). Risk, by contrast, incorporates the exposure of people and assets to those hazardous conditions. The distinction between susceptibility and risk is particularly important in rapidly urbanising districts such as Kolhapur, where the growth of impervious surfaces and population concentration in flood-prone zones has progressively amplified vulnerability.

This study addresses that gap by presenting a geospatial flood risk assessment for Kolhapur district integrating: (i) mean annual rainfall from CHIRPS, (ii) terrain slope from SRTM DEM, (iii) urban density from built-up classification, and (iv) gridded population count (WorldPop). The specific objectives are: (i) to map and analyse flood susceptibility; (ii) to derive and classify a population-weighted flood risk index;

ISSN (Online) 2456-1290

International Journal of Engineering Research in Mechanical and Civil Engineering (IJERMCE)

Volume 13, Issue 06, June 2026

(iii) to examine statistical relationships between flood drivers and risk; and (iv) to identify high-risk spatial clusters.

II. NEED OF THE STUDY

Kolhapur district has experienced recurrent and increasingly severe flood events, most notably in 2019 and 2021, which caused widespread loss of life, destruction of agricultural land, and disruption of urban infrastructure. Despite the severity of these events, no comprehensive, spatially explicit flood risk assessment integrating multiple biophysical and socio-demographic parameters has been conducted for the district at a systematic level. This study directly addresses that need by combining open-source geospatial data with a multi-criteria risk index framework to produce actionable flood risk maps for Kolhapur district.

III. METHODOLOGY

The methodological workflow follows a sequential geospatial analysis framework proceeding from data acquisition and pre-processing through composite index computation to spatial classification and statistical validation. The overall approach is: Data Acquisition → Pre-processing & Normalisation → FSI Computation → FRI Computation → Spatial Classification → Statistical Analysis → Flood Risk Maps.

IV. STUDY AREA

Kolhapur district is located in the southern part of Maharashtra state, India, between approximately 15°48′N to 17°02′N latitude and 73°38′E to 74°53′E longitude. The district covers an area of approximately 7,685 km² and is bounded by the Sahyadri (Western Ghats) mountain ranges to the west, which trigger extremely heavy monsoon rainfall on the windward slopes. The Panchganga River and its tributaries form the principal drainage network.

The topography of Kolhapur is highly varied, transitioning from steep hillslopes in the western Sahyadri zone (elevations exceeding 900 m msl) to broad alluvial plains in the central and eastern parts (450–600 m msl). Mean annual rainfall ranges from approximately 17,000 mm in the extreme western high-altitude zones to below 20,000 mm in rain-shadow areas to the east, following a pronounced east-west gradient. The summer monsoon (June to September) accounts for over 90% of annual precipitation. The Kolhapur Municipal Corporation (KMC) area constitutes the primary urban nucleus, with a population of approximately 550,000 as of the 2011 Census (Census of India, 2011; Municipal Corporation of Kolhapur, 2022).

V. TOOLS AND TECHNIQUES

This study employed a Python 3.10-based geospatial processing environment using: rasterio for raster I/O and CRS management; numpy for array-level arithmetic; scipy for statistical computations; and matplotlib for visualisation. Spatial data were managed in the WGS 84 / UTM Zone 43N projected coordinate system. All raster layers were resampled to a common 500 m spatial resolution using bilinear interpolation. The four key parameters were individually normalised using min-max scaling prior to index computation, consistent with established approaches (Samanta et al., 2018; Tehrany et al., 2014).

5.1. Data Pre-Processing and Normalisation

All raster datasets were projected to WGS 84 / UTM Zone 43N and resampled to ~500 m using bilinear interpolation. Pixel-wise normalisation was applied using min-max scaling:

$$\mathbf{X_n = (X - X_{min}) / (X_{max} - X_{min})}$$

For terrain slope, the normalised value was inverted ($1 - slope_n$) so that low-gradient areas receive higher susceptibility scores. NoData and zero-rainfall pixels were excluded from all analyses.

5.2. Flood Susceptibility Index (FSI) Computation

Flood susceptibility was computed as a weighted linear combination of normalised rainfall (rainN) and inverted normalised slope (slopeN_inv):

$$\mathbf{FSI = \alpha \times rainN + \beta \times slopeN\_inv}$$

where $\alpha = 0.6$ and $\beta = 0.4$, reflecting the dominant role of precipitation intensity as a flood driver in the Kolhapur context, consistent with Samanta et al. (2018). The resulting FSI ranges from 0 (minimum) to 1 (maximum susceptibility).

5.3. Flood Risk Index (FRI) Computation

Flood risk was operationalised as the product of susceptibility and a composite vulnerability-exposure term:

$$\mathbf{FRI = FSI \times [\gamma \times popN + \delta \times urbanN]}$$

where $\gamma = \delta = 0.5$, assigning equal weight to population density and urban cover. This formulation ensures that physically susceptible but unpopulated areas receive low risk scores. The FRI was subsequently rescaled to 0–1 and classified into three quantile-based risk classes (Low = Class 1, Moderate = Class 2, High = Class 3).

5.4. Statistical and Spatial Analysis

Frequency distributions of FSI and FRI were examined through histograms. Bivariate scatter plots explored relationships between flood risk and individual driving variables (rainfall, urban density) and between FSI and FRI. A box plot compared normalised rainfall in urban versus non-urban areas. All analyses were performed in Python 3.10.

VI. DATA COLLECTION

Four datasets were used: (i) Rainfall — mean annual precipitation from CHIRPS v2.0 at 0.05° resolution; (ii) Terrain Slope — derived from SRTM 30 m DEM; (iii) Urban Density — binary urban/non-urban classification normalised to 0–1; and (iv) Population — WorldPop gridded population

ISSN (Online) 2456-1290
International Journal of Engineering Research in Mechanical and Civil Engineering (IJERMCE)
Volume 13, Issue 06, June 2026

counts at 100 m resolution, resampled to match the working grid.

VII. DATA ASSESSMENT AND ANALYSIS

7.1. Spatial Distribution of Input Variables

Figure 1 presents the spatial distribution of urban density across Kolhapur district. The most densely built-up areas (urban density = 1.0) are concentrated in the central-northern zone corresponding to Kolhapur city and its immediate periphery, reflecting recent urban sprawl along major road corridors. The southern and western zones are predominantly rural or forested with near-zero urban density.

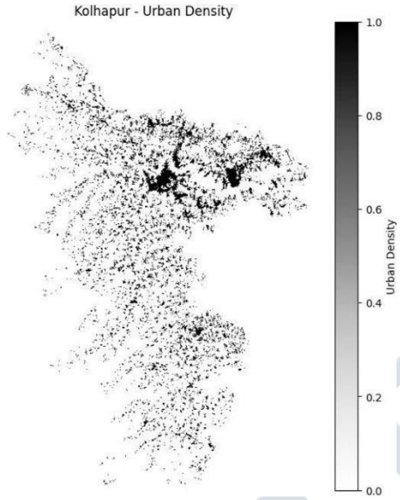

Fig. 1. Spatial distribution of urban density across Kolhapur district

Figure 2 illustrates terrain slope in degrees. The western Sahyadri escarpments exhibit the steepest slopes (20–40°). The central and eastern portions are dominated by gentle slopes (0–10°), representing alluvial plains and low terraces along the Panchganga River — the primary areas of flood inundation during peak monsoon discharge.

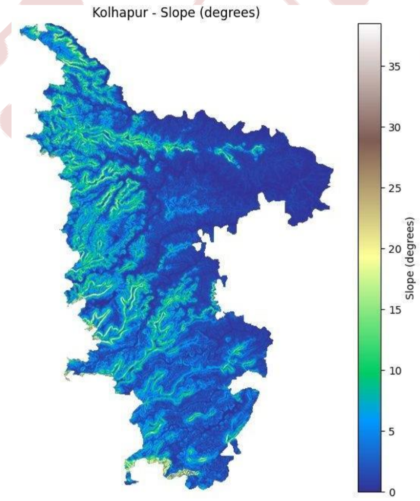

Fig. 2. Terrain slope (degrees) derived from SRTM 30 m DEM, Kolhapur district

Figure 3 shows the gridded population distribution highlighting strong spatial concentration in the Kolhapur urban agglomeration (pixel counts exceeding 160 persons per grid cell). The remainder of the district has a dispersed rural population pattern, with moderate densities in the talukas of Ichalkaranji, Kagal, and Jaysingpur.

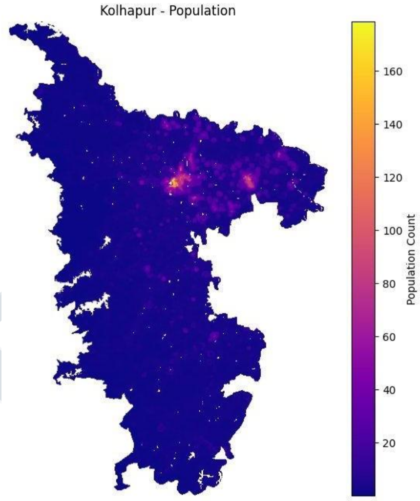

Fig. 3. Gridded population count, Kolhapur district (WorldPop dataset)

The mean annual rainfall map Fig. 4 reveals a pronounced east-west gradient: westernmost pixels exceed 60,000 mm (pixel-aggregated values at working resolution) while eastern portions receive 17,000–25,000 mm. This gradient is the dominant forcing variable for flood susceptibility across western portions of the district.

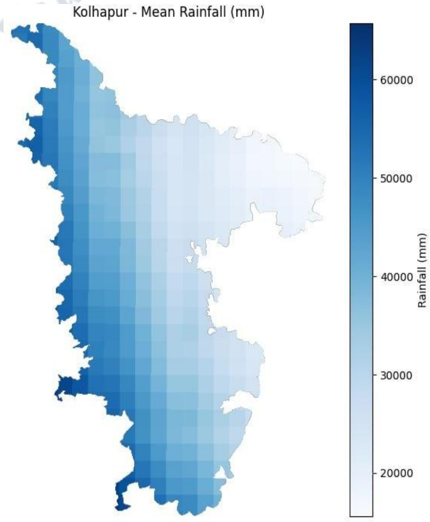

Fig. 4. Mean annual rainfall distribution (mm) across Kolhapur district

7.2. Flood Susceptibility Index

The spatial pattern of the Flood Susceptibility Index (Figure 5) reflects the combined influence of rainfall and inverse slope. The western Sahyadri zone shows moderately elevated susceptibility due to the dampening effect of steep

ISSN (Online) 2456-1290

International Journal of Engineering Research in Mechanical and Civil Engineering (IJERMCE)

Volume 13, Issue 06, June 2026

slopes. The highest susceptibility values (FSI > 0.7) are concentrated in the central and northeastern zones where relatively high rainfall coincides with gentle alluvial gradients.

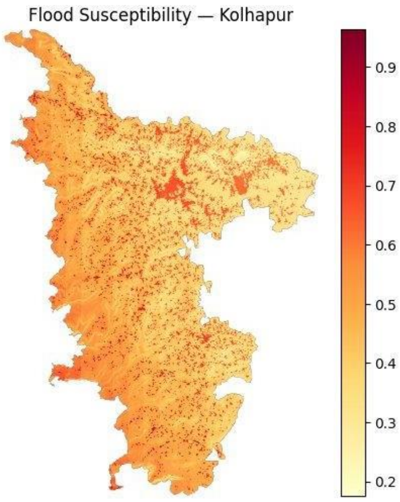

Fig. 5. Flood Susceptibility Index (FSI), Kolhapur district

The frequency distribution of FSI values (Figure 6) shows a unimodal distribution centred at FSI ≈ 0.40–0.45, with a pronounced right tail to FSI ≈ 1.0. Approximately 60% of district pixels fall within the moderate susceptibility range (FSI = 0.30–0.55). Only ~5% exhibit high susceptibility (FSI > 0.70), concentrated in urban plains and riverine corridors.

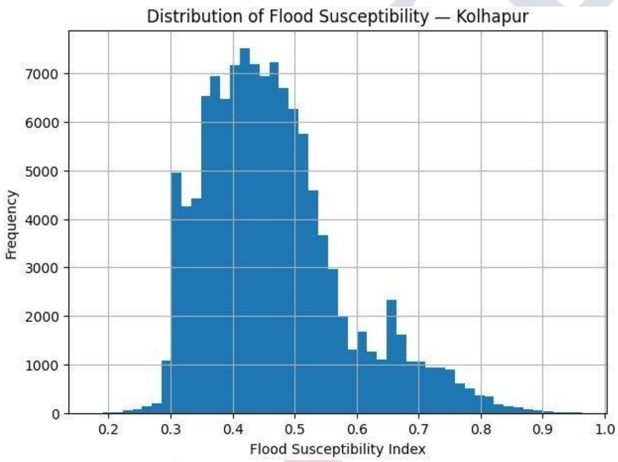

Fig. 6. Frequency distribution of Flood Susceptibility Index (FSI) values, Kolhapur district

7.3. Flood Risk Index and Classification

The Flood Risk Index map (Figure 7) demonstrates a dramatically different spatial pattern compared to susceptibility alone. The majority of the district (≥90% of land pixels) exhibits near-zero flood risk, reflecting the sparsely populated nature of rural and forested zones. The Kolhapur Municipal Corporation area displays a distinctive high-risk nucleus with FRI values ranging from 0.3 to 0.65, corresponding to the convergence of moderate-to-high susceptibility with highest population densities.

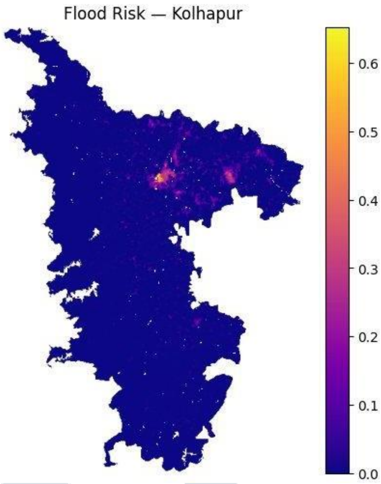

Fig. 7. Flood Risk Index (FRI), Kolhapur district

The rescaled flood risk map (Figure 8) confirms that the top 10–15% of risk values are spatially concentrated in approximately 200–300 km² centred on the urban core. The quantile classification (Figure 9) identifies a substantial moderate-risk zone (Class 2, green) covering most inhabited portions, with the high-risk class (Class 3, yellow) isolated within the principal urban agglomeration.

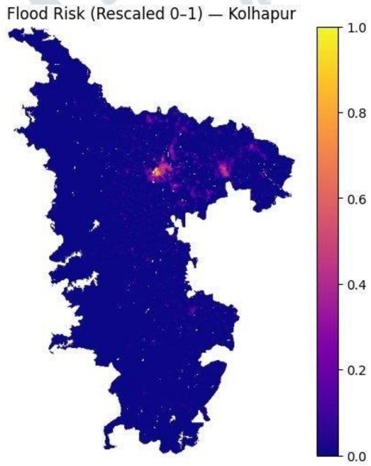

Fig. 8. Flood Risk Index rescaled (0–1), Kolhapur district

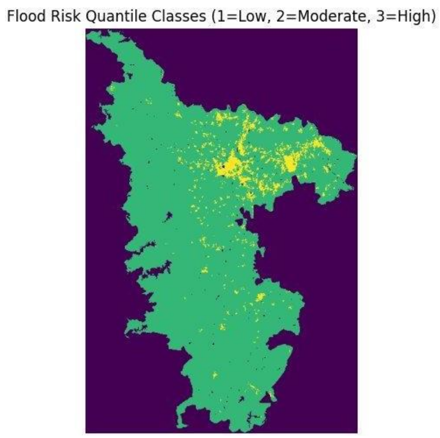

Fig. 9. Quantile-based flood risk classification (1 = Low, 2 = Moderate, 3 = High), Kolhapur district

The frequency distribution of FRI values (Figure 10) is heavily right-skewed, with a dominant spike at FRI ≈ 0.00–0.02 accounting for over 110,000 pixels. The small fraction of pixels with FRI > 0.05 constitutes the high-risk population cluster and represents the primary target for flood risk management interventions.

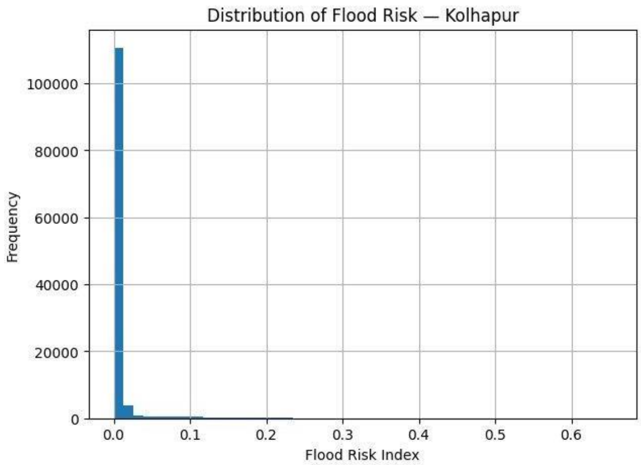

Fig. 10. Frequency distribution of Flood Risk Index (FRI) values, Kolhapur district

7.4. Relationships Between Flood Drivers and Risk

The scatter plot of FSI versus FRI (Figure 11) reveals a striking threshold pattern: flood risk remains near zero for all pixels with FSI < 0.60, irrespective of susceptibility magnitude. Above FSI ≈ 0.62–0.65, FRI values spike sharply, producing a near-vertical cluster of high-risk pixels. This threshold behaviour is consistent with urban imperviousness theories associating rapid runoff generation with built-up surfaces above a critical coverage fraction.

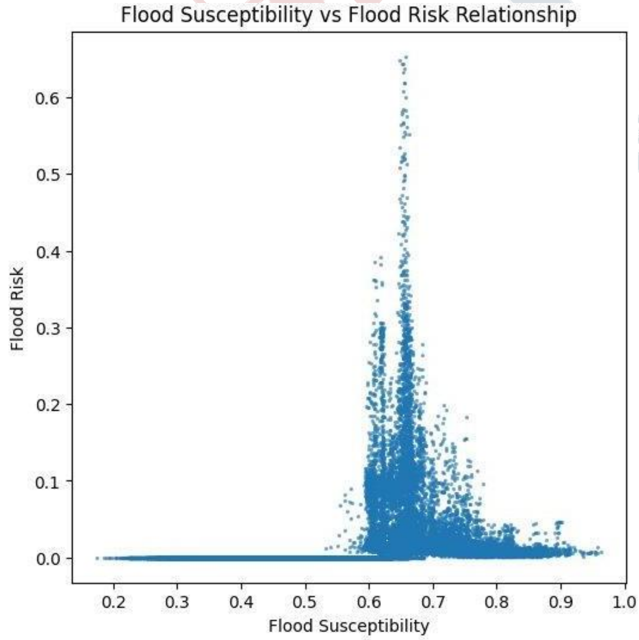

Fig. 11. Flood Susceptibility vs. Flood Risk scatter plot, Kolhapur district

The scatter plot of rainfall versus flood risk (Figure 12) shows maximum risk values (≈0.65) occurring at intermediate rainfall totals (≈25,000 mm) rather than at peak rainfall. This counterintuitive result reflects the spatial decoupling of maximum rainfall (concentrated in steep, unpopulated western slopes) from maximum population density (concentrated in lower-rainfall central plains).

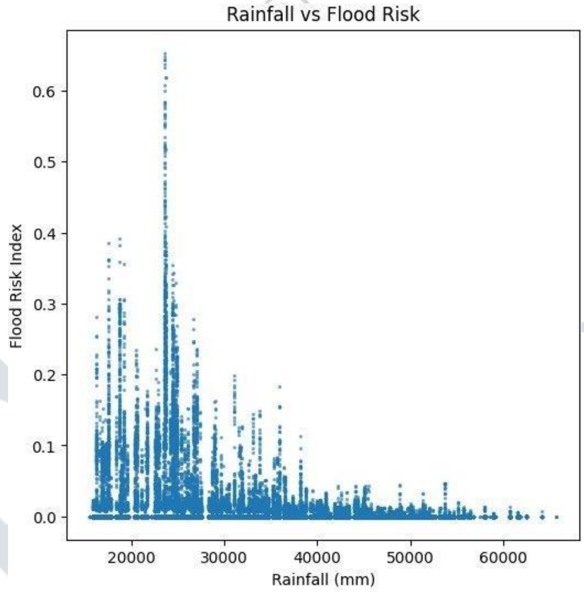

Fig. 12. Rainfall vs. Flood Risk Index scatter plot, Kolhapur district

The scatter plot of urban density versus flood risk (Figure 13) demonstrates that essentially all high-risk pixels (FRI > 0.1) are confined to grid cells with urban density = 1.0, while zero-urban-density pixels universally exhibit near-zero flood risk, confirming that urban cover is a necessary condition for high flood risk in Kolhapur.

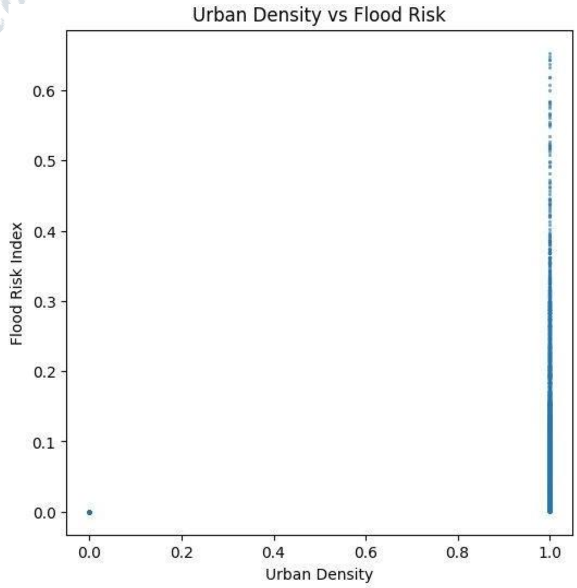

Fig. 13. Urban density vs. Flood Risk Index scatter plot, Kolhapur district

IFERP Explore Your Research Journey...
ISSN (Online) 2456-1290
International Journal of Engineering Research in Mechanical and Civil Engineering (IJERMCE)
Volume 13, Issue 06, June 2026

VIII. DISCUSSION

The results advance understanding of flood risk dynamics in Kolhapur along several dimensions. First, the spatial concentration of flood risk in the urban core contrasts sharply with the broad distribution of flood susceptibility, highlighting the critical role of population exposure and urban density as amplifiers of hazard into risk, consistent with global urban flood risk literature (Jha et al., 2012; Hallegatte et al., 2013).

Second, the threshold behaviour observed in the FSI-FRI relationship (Figure 11) has important methodological implications. The sharp activation of flood risk above FSI ≈ 0.62 suggests that a binary categorisation of susceptibility may be more informative for risk communication than the full continuous index. Third, the finding that maximum flood risk occurs at intermediate rather than maximum rainfall totals has implications for early warning system design; alerts should be calibrated to urban-specific susceptibility thresholds rather than district-wide maximum rainfall.

Fourth, the lower median rainfall in urban areas relative to non-urban areas (Figure 14) has implications for climate change projections. If future scenarios project intensification of rainfall in the western Sahyadri, the impact on urban flood risk will be mediated through catchment routing. Projections of increased extreme rainfall events at moderate intensities in the central plains would directly amplify flood risk in the urban core.

The methodology carries several limitations. The weighted index approach does not account for hydrological connectivity, channel routing, or flood stage-discharge relationships. The use of CHIRPS mean annual rainfall may smooth out extreme event intensities that drive flood peaks. Future work should integrate hydraulic models, soil type, drainage network density, antecedent soil moisture, and land-use change projections (Tehrany et al., 2019; Bera et al., 2021).

IX. CONCLUSION

This study presents a comprehensive geospatial flood risk assessment for Kolhapur district, integrating terrain slope, mean annual rainfall, urban density, and gridded population count within a multi-criteria weighted index framework. The principal findings are:

(i) Flood susceptibility across Kolhapur is moderately high (mean FSI ≈ 0.45) and broadly distributed, with highest values in the low-gradient central plains. (ii) Flood risk is highly spatially concentrated in the Kolhapur Municipal Corporation area; the majority of the district (≥90% of land pixels) exhibits negligible flood risk. (iii) Flood risk exhibits a non-linear threshold response to susceptibility, activating sharply at FSI ≈ 0.62–0.65, corresponding to fully urbanised pixels with maximum population density. (iv) Maximum flood risk does not coincide with maximum rainfall but with intermediate rainfall co-located with high urban density and population. (v) Urban areas are systematically located in lower-rainfall zones, indicating that urban flood risk is driven primarily by concentrated upstream runoff and reduced infiltration rather than direct local precipitation extremes.

Priority interventions should target the high-risk urban nucleus through enhanced stormwater drainage, flood-proofing of low-income settlements in floodplain zones, and real-time early warning systems calibrated to urban-specific susceptibility thresholds. The open-source geospatial framework is transferable to other rapidly urbanising districts in Maharashtra and the Western Ghats region.

X. INTERVENTIONS AND FUTURE OUTCOMES

Based on the findings of this study, the following proposals are recommended: (i) Priority infrastructure investment should focus on enhanced stormwater drainage systems and retention ponds in high-risk peri-urban zones. (ii) Real-time flood early warning systems, calibrated to the urban-specific threshold of FSI ≈ 0.62, should be developed and integrated with India Meteorological Department monitoring. (iii) Zoning regulations should restrict further residential development in quantile Class 3 risk areas, particularly in low-gradient floodplain zones adjacent to the Panchganga River. (iv) Community-level flood preparedness programmes targeting informal settlements in the high-risk urban nucleus are strongly recommended.

Future research should: integrate hydraulic routing models (HEC-RAS, LISFLOOD) for dynamic flood extent predictions; incorporate soil type, drainage network density, antecedent soil moisture, and land-use change trajectories; conduct temporal analysis using multi-decadal rainfall records; and scale the framework to other flood-prone districts of Maharashtra.

Competing Interests

Authors have declared that no competing interests exist.

REFERENCES

[1] Bera, S., Das Chatterjee, N., & Bera, S. (2021). Soil erosion mapping and vulnerability analysis in a flood-prone district of West Bengal, India using geospatial techniques. Geocarto International, 36(12), 1312–1336. https://doi.org/10.1080/10106049.2019.1648930

[2] Census of India. (2011). District Census Handbook: Kolhapur. Office of the Registrar General and Census Commissioner, India.

[3] Chen, W., Li, Y., Xue, W., Shahabi, H., Li, S., Hong, H., & Ahmad, B. B. (2020). Modeling flood susceptibility using data-driven approaches of naive Bayes tree, alternating decision tree, and random forest methods. Science of the Total Environment, 701, 134979. https://doi.org/10.1016/j.scitotenv.2019.134979

[4] Costache, R., & Tehrany, M. S. (2019). Rainfall-induced flash flood potential assessment at the intersection of the Eastern Carpathians with the Siret River, Romania. Water Resources Management, 33(7), 2511–2527. https://doi.org/10.1007/s11

269-019-02268-1

[5] Dhar, O. N., & Nandargi, S. (2003). Hydrometeorological aspects of floods in India. Natural Hazards, 28(1), 1–33. https://doi.org/10.1023/A:1021199714487

[6] Farr, T. G., Rosen, P. A., Caro, E., Crippen, R., Duren, R., Hensley, S., & Alsdorf, D. (2007). The Shuttle Radar Topography Mission.

[7] Reviews of Geophysics, 45(2), RG2004. https://doi.org/10.1029/2005RG000183

[8] Funk, C., Peterson, P., Landsfeld, M., Pedreros, D., Verdin, J., Shukla, S., & Michaelsen, J. (2015). The climate hazards infrared precipitation with stations — a new environmental record for monitoring extremes. Scientific Data, 2, 150066. https://doi.org/10.1038/sdata.2015.66

[9] Hallegatte, S., Green, C., Nicholls, R. J., & Corfee-Morlot, J. (2013). Future flood losses in major coastal cities. Nature Climate Change, 3(9), 802–806. https://doi.org/10.1038/nclimate1979

[10] Jha, A. K., Bloch, R., & Lamond, J. (2012). Cities and flooding: A guide to integrated urban flood risk management for the 21st century.

[11] World Bank Publications. https://doi.org/10.1596/978-0-8213-8866-2

[12] Khosravi, K., Nohani, E., Maroufinia, E., & Pourghasemi, H. R. (2016). A GIS-based flood susceptibility assessment and its mapping in Iran. Natural Hazards, 83(2), 947–987. https://doi.org/10.1007/s11069-016-2357-2

[13] Municipal Corporation of Kolhapur. (2022). City Development Plan. Kolhapur: Municipal Corporation of Kolhapur.

[14] Nandi, A., Mandal, A., Wilson, M., & Smith, D. (2016). Flood hazard mapping in Jamaica using principal component analysis and logistic regression. Environmental Earth Sciences, 75(6), 465. https://doi.org/10.1007/s12665-016-5323-0

[15] Pradhan, B. (2010). Flood susceptible mapping and risk area delineation using logistic regression, GIS and remote sensing. Journal of Spatial Hydrology, 9(2), 1–18.

[16] Rahmati, O., Pourghasemi, H. R., & Zeinivand, H. (2016). Flood susceptibility mapping using frequency ratio and weights-of-evidence models in the Golastan Province, Iran. Geocarto International, 31(1), 42–70. https://doi.org/10.1080/10106049.2015.1041559 Samanta, S., Pal, D. K., & Palsamanta, B. (2018). Flood susceptibility analysis through remote sensing, GIS and frequency ratio model.

[17] Applied Water Science, 8(2), 66. https://doi.org/10.1007/s13201-018-0710-1

[18] Sanyal, J., & Lu, X. X. (2004). Application of remote sensing in flood management with special reference to monsoon Asia: A review.

[19] Natural Hazards, 33(2), 283–301. https://doi.org/10.1023/B:NHAZ.0000037035.65105.95

[20] Sinha, R., Bapalu, G. V., Singh, L. K., & Rath, B. (2008). Flood risk analysis in the Kosi river basin, North Bihar using multi-parametric approach of analytical hierarchy process (AHP). Journal of the Indian Society of Remote Sensing, 36(4), 335–349. https://doi.org/10.1007/s12524-008-0034-y

[21] Tehrany, M. S., Pradhan, B., & Jebur, M. N. (2014). Flood susceptibility mapping using a novel ensemble weights-of-evidence and support vector machine models in GIS. Journal of Hydrology, 512, 332–343. https://doi.org/10.1016/j.jhydrol.2014.03.008

[22] Tehrany, M. S., Jones, S., Shabani, F., Martínez-Álvarez, F., & Bui, D. T. (2019). A novel ensemble modeling approach for the spatial prediction of tropical forest fire susceptibility. Theoretical and Applied Climatology, 137(1), 637–653. https://doi.org/10.1007/s00704-018-2638-9

[23] UNDRR. (2020). The Human Cost of Disasters: An Overview of the Last 20 Years (2000–2019). United Nations Office for Disaster Risk Reduction, Geneva. https://www.undrr.org/publication/human-cost-disasters-overview-last-20-years-2000-2019

[24] Vojtek, M., & Vojteková, J. (2019). Flood susceptibility mapping on a national scale in Slovakia using the analytical hierarchy process.

[25] Water, 11(2), 364. https://doi.org/10.3390/w11020364

[26] WorldPop. (2020). Population Count. WorldPop, University of Southampton, UK. https://www.worldpop.org/